

# Card-type Piezoelectric Energy Harvesters of Pb(Zr,Ti)O<sub>3</sub> Thin Films on Stainless Steel Foils

Daiki Teramoto, SangHyo Kweon, and Isaku Kanno\*

Department of Mechanical Engineering, Kobe University,  
1-1 Rokkodai-cho, Nada-ku, Kobe 657-8501, Japan

(Received November 29, 2023; accepted December 25, 2023)

**Keywords:** energy harvesting, piezoelectric, PZT thin film, flexible

In this study, we fabricated flexible card-type piezoelectric energy harvesters (PEHs) composed of Pb(Zr,Ti)O<sub>3</sub> (PZT) thin films on stainless steel foils for wearable applications and measured their power generation performance under hand-bending motion. The PZT thin films with preferential c-axis orientation were deposited on LaNiO<sub>3</sub> (LNO)-coated stainless steel substrates of 30 μm in thickness by RF magnetron sputtering. Five PZT thin-film PEH elements were stacked with each connected in parallel. The stack was placed in the middle of a card divided into two parts. We measured the output power while applying a large hand-bending deformation to the card-type PEHs. During periodic bending motion at 1 Hz the maximum output power reached 177 μW at a load resistance of 80 kΩ, and we successfully turned 10 LEDs on intermittently.

## 1. Introduction

In recent years, the practical application of wearable devices as next-generation functional devices in which microsensors and actuators are attached to the body has attracted attention.<sup>(1–4)</sup> One of the problems in the practical application of wearable devices is the difficulty in supplying electric power from a grid power source without restricting human mobility. Wearable devices are usually powered by portable batteries; however, there is strong demand to realize battery-free wearable devices with a self-power generator that converts dilute energy in the environment into electrical energy.<sup>(5,6)</sup> Piezoelectric energy harvesting is a power generation method suitable as an independent small-scale power source for wearable devices because of the simple structure and easy miniaturization of piezoelectric energy harvesters (PEHs), which have been investigated for practical application.<sup>(7–11)</sup>

In our previous study, we fabricated glove-type PEHs that were attached to finger joints and generated electric power from finger flexion motion.<sup>(12)</sup> In that study, piezoelectric Pb(Zr,Ti)O<sub>3</sub> (PZT) thin films, which were deposited on stainless steel foils by RF magnetron sputtering, were used for fabricating PEHs, and piezoelectric power elements with flexibility and durability in addition to good piezoelectric properties were realized. The glove-type PEHs generated a

---

\*Corresponding author: e-mail: [kanno@mech.kobe-u.ac.jp](mailto:kanno@mech.kobe-u.ac.jp)  
<https://doi.org/10.18494/SAM4810>

maximum output power of 13.4  $\mu\text{W}$  by finger flexion motion, which we successfully used to turn on an LED intermittently.

In this study, we investigated the improvement in power generation performance and new applications of PZT thin-film power generation devices on stainless steel. As a new application device of PEHs consisting of PZT thin-film foils, we fabricated card-type PEHs for a self-powered smart card. For example, typical credit cards or RF tags are equipped with electronic devices such as IC chips and memory functions; however, the small thickness of the card itself makes it difficult to mount a battery, and electric power for reading and writing information is supplied by contact or electromagnetic waves. However, if these IC cards and tags are self-powered, new applications can be expected, such as the ability to read, write, and transmit information at any location. For power generation by direct hand-bending action, flexible and high-power PEHs must be integrated into smart cards. In this study, we applied our above-mentioned technology of a flexible PZT thin-film generator using a PZT thin film on a stainless steel foil to card-type PEHs. Furthermore, to improve the power generation performance, we investigated the effect of orientation control by introducing a buffer layer between the substrate and the PZT thin film in the sputter deposition process.

## 2. Experimental Procedure

### 2.1 Single PEH element

A PZT thin film was deposited on a 30- $\mu\text{m}$ -thick stainless steel foil (SUS430) by RF magnetron sputtering to fabricate a card-type PEH. Figure 1 illustrates the fabrication process for a single element of the PEH. We deposited Pt/Ti on a stainless steel foil as a bottom electrode, followed by a 40-nm-thick  $\text{LaNiO}_3$  (LNO) buffer layer to improve the growth of the PZT thin film with preferential c-axis orientation.<sup>(13)</sup> After that, a PZT thin film of 5.0  $\mu\text{m}$  thickness was deposited as a piezoelectric layer. A Pt top electrode with an area of 380  $\text{mm}^2$  was deposited on the surface of the PZT thin film using a shadow mask. Figure 2 shows a photograph and a schematic illustration of the PEH element composed of a PZT thin film on a stainless steel foil. For use as a multielement PEH, a fluorine tape (ASF-110, Chukoh Chemical Industries, Ltd.) was attached to the Pt top electrode as a protective and insulating layer to prevent damage due to contact between adjacent PEH elements. The crystal structure of the PZT thin film was measured by X-ray diffraction (XRD), and its dielectric properties were measured using an LCR meter (NF, ZN2353).

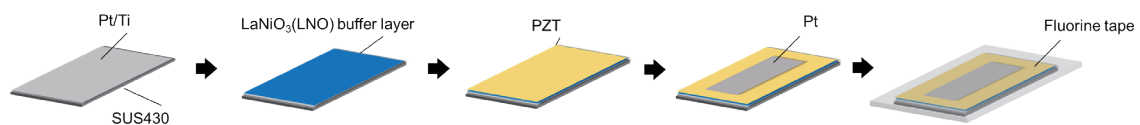


Fig. 1. (Color online) Fabrication process for energy harvester.

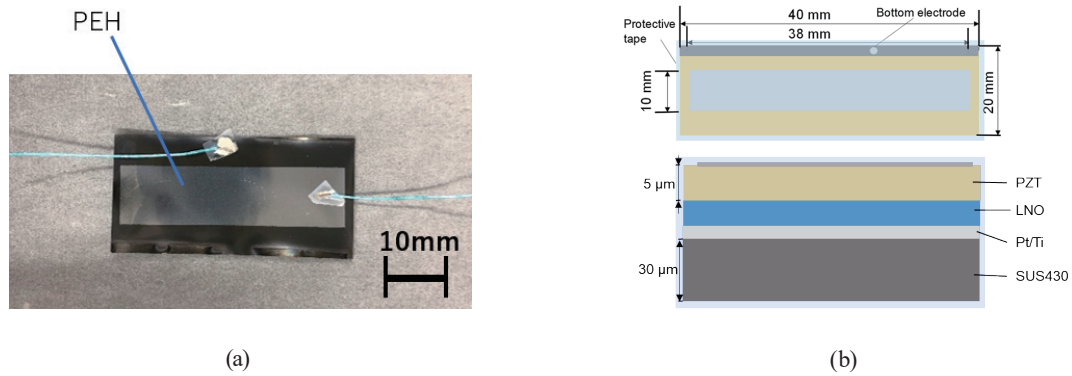


Fig. 2. (Color online) Piezoelectric thin-film energy harvester: (a) optical photograph and (b) surface and cross-sectional structure.

## 2.2 Card-type PEH

The card-type generator must be installed in the narrow space of the card, but the area allowed for the PEH is very small. Therefore, in this study, to increase the effective area of the PEH, five elements were stacked and connected in parallel, and then installed in the middle of a card divided into two parts. Figure 3 shows photographs and schematics of the card-type PEH using a PZT thin film on a stainless steel foil.

Next, we measured the output power of the card-type PEH via hand-bending motion with a frequency of about 1 Hz. The bending angle of the PEH was about  $115^\circ$ , which corresponds to a 0.38% strain on the PZT thin film on the stainless steel foil. We connected a variable resistor in parallel between the top and bottom electrodes of the card-type PEH. When the PEH was bent by hand, the output voltage at the load resistance was measured using an oscilloscope (GDS1062A, NF). The output power  $P$  was derived using

$$P = \frac{1}{T} \int \frac{V(t)^2}{R} dt, \quad (1)$$

where  $T$  is the bending period,  $V(t)$  is the output voltage, and  $R$  is the load resistance. After that, we demonstrated the lighting of LEDs to test the power supply capability of the card-type PEH by connecting it to an energy-harvesting module (LTC3588-1) to rectify the output voltage of the card-type PEH.

## 3. Results and Discussion

### 3.1 Single PEH element

Figure 4 shows the XRD pattern of a PZT thin film on a stainless steel foil with the LNO buffer layer. The XRD measurements indicated that the crystal structure of the PZT thin film had a strong c-axis orientation due to the LNO buffer layer. The relative dielectric constant and

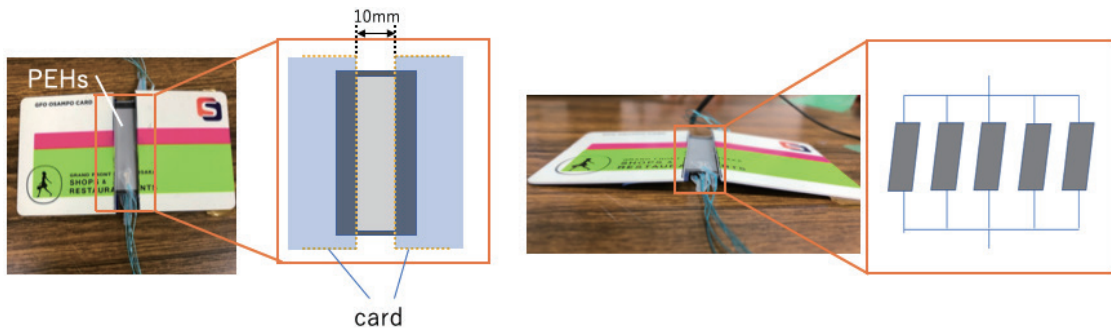


Fig. 3. (Color online) Optical photographs and schematics of card-type PEH.

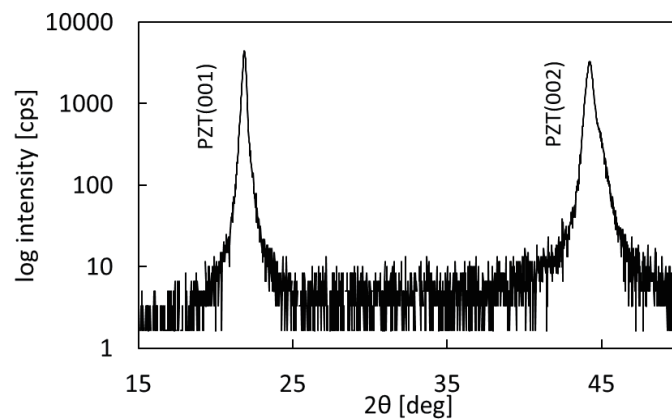
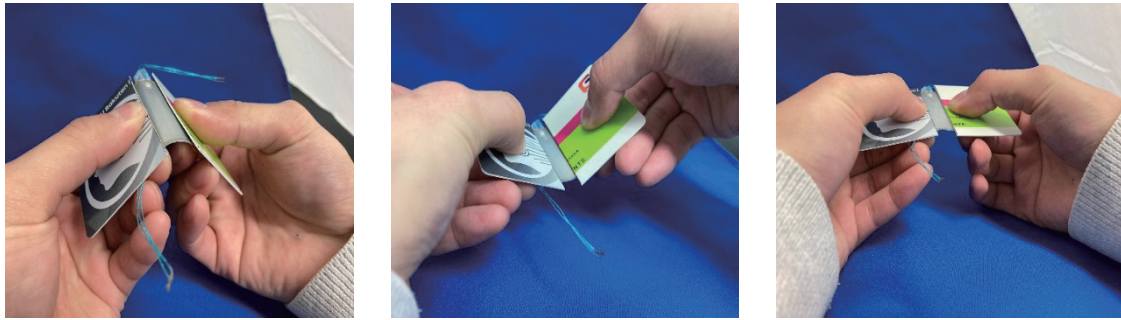


Fig. 4. XRD pattern of PZT thin film deposited on 30- $\mu\text{m}$ -thick SUS430 foil with LNO buffer layer.

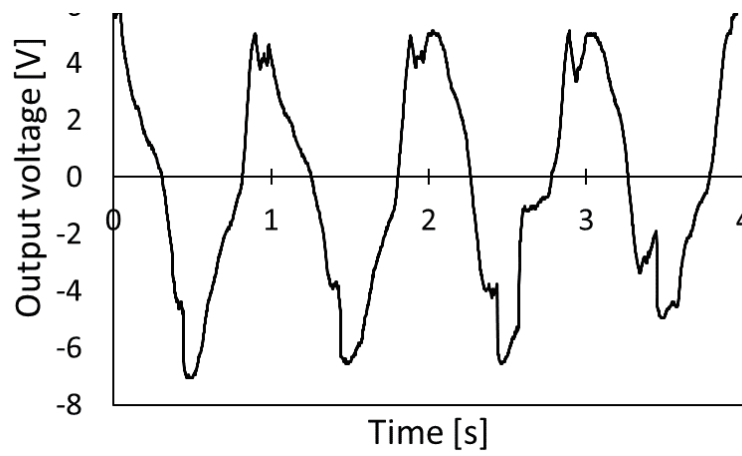
dielectric loss of a single PEH element were 177.1–223.0 and less than 6%, respectively, indicating that the fabricated single PEH element had satisfactory insulating properties. The transverse piezoelectric coefficient  $|e_{31,f}|$  was measured from the direct piezoelectric effect of PZT thin films used in the PEH, and the relatively large value of around  $6.5 \text{ C/m}^2$  was obtained. This value was almost the same as the direct piezoelectric coefficient  $|e_{31,f}|$  of polycrystalline PZT thin films on Si.<sup>(14)</sup>

### 3.2 Card-type PEH

The five PEH elements connected in parallel had a capacitance and dielectric loss of  $1.03 \mu\text{F}$  and 7.3%, respectively. Figure 5 shows the output voltage during output measurement when the card-type PEH was manually bent at 1 Hz. Although the output voltage is not an ideal sinusoidal wave, the approximate output performance is estimated as a sinusoidal voltage. Figure 6 shows the output voltage and power of the card-type PEH during hand-bending motion at 1 Hz. The maximum output power  $P$  reached  $177 \mu\text{W}$ , that is,  $177 \mu\text{J}$  for each bending operation, at a load resistance of  $80 \text{ k}\Omega$ . For comparison, a card-shaped PEH with the same structure was fabricated



(a)



(b)

Fig. 5. (Color online) Manual bending operation during output power measurement of card-type PEH. (a) Pictures of bending operation and (b) output voltage.

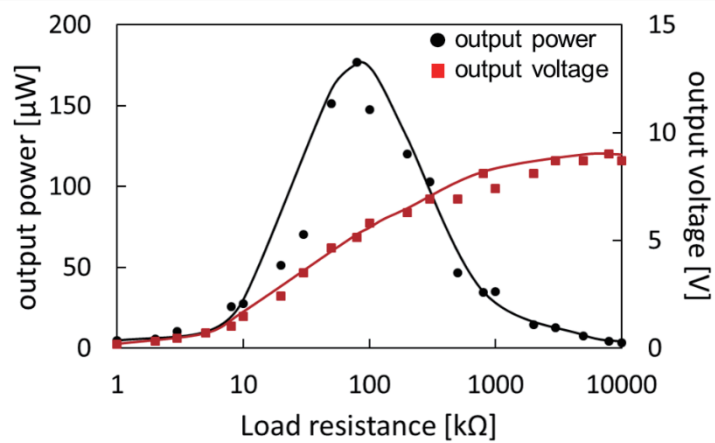


Fig. 6. (Color online) Output voltage and output power of PEH as a function of load resistance.

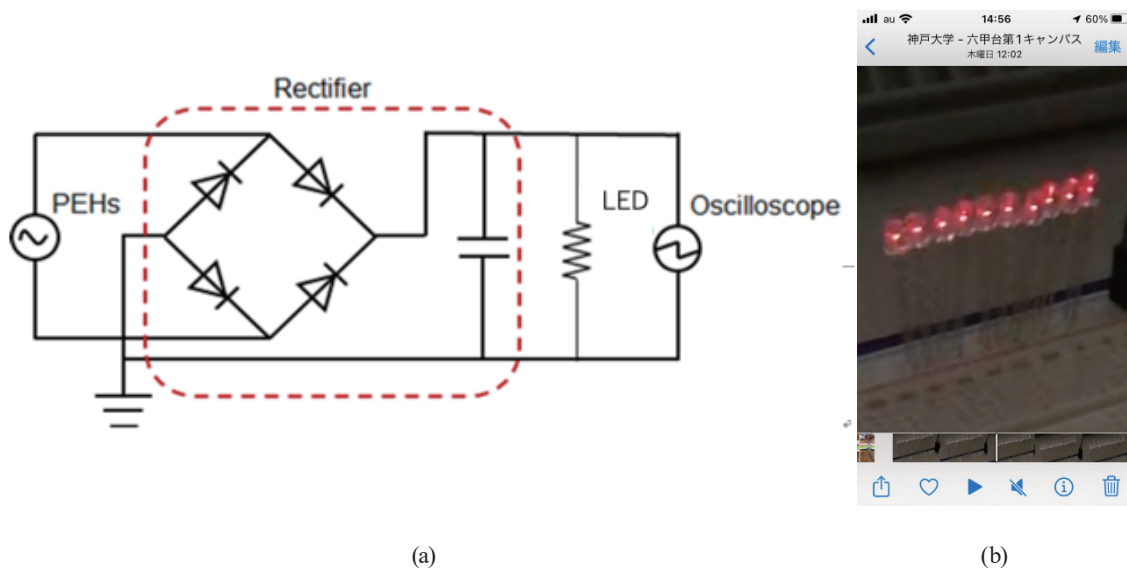


Fig. 7. (Color online) (a) Measurement system of output power of PEH to turn on LEDs and charge battery. (b) Photograph of 10 LEDs turned on.

using a randomly oriented PZT thin film, and its maximum output power was measured to be  $66 \mu\text{W}$ . Thus, the output power of the card-type PEH with c-axis oriented PZT thin films was approximately 2.5 times higher than that of the card-type PEH with randomly oriented PZT thin films. These results indicate that the output power of the card-type PEH strongly depends on the orientation of the PZT thin films and that the LNO buffer layer is effective in aligning the orientation of the PZT thin film with the c-axis.

Next, we conducted an LED lighting test using the generated output power to demonstrate the practicality of the card-type PEH. The output terminal of the PEH was connected to a commercially available energy-harvesting module (LTC3588-1). Upon rectifying the power obtained from the manual bending deformation, the output voltage was 3 V, and a constant voltage was continuously extracted. Figure 7 shows a schematic of the LED lighting circuit and an optical photograph of the LEDs lit via the bending of the card-type PEH. We succeeded in lighting 10 LEDs intermittently with hand-bending motion of the PEH, confirming its capability of generating a significant electric power.

#### 4. Conclusion

In this study, we fabricated card-type PEHs via hand-bending motion. Their elements were composed of PZT thin films deposited on  $30\text{-}\mu\text{m}$ -thick SUS430 foils by RF magnetron sputtering. The fabricated PZT thin films had a c-axis orientation due to the LNO buffer layer. Five PZT thin-film PEH elements were stacked, with each connected in parallel, to improve the output voltage and output power of the PEH. During hand-bending motion at 1 Hz, the maximum output power  $P$  was  $177 \mu\text{W}$  at a load resistance of  $80 \text{ k}\Omega$ . The output power of the card-type

PEH with c-axis oriented PZT thin films was approximately 2.5 times higher than that of the card-type PEH with randomly oriented PZT thin films. Using the rectified output power of the card-type PEH, we successfully turned on 10 LEDs.

### Acknowledgments

This study was supported by Japan Science and Technology Agency projects of CREST (JPMJCR20Q2).

### References

- 1 Y. Cheng, K. Wang, H. Xu, T. Li, Q. Jin, and D. Cui: *Anal. Bioanal. Chem.* **413** (2021) 6037. <https://doi.org/10.1007/s00216-021-03602-2>
- 2 N. Shenck and J. Paradiso: *IEEE Micro.* **21** (2001) 30. <https://doi.org/10.1109/40.928763>
- 3 T. Ghomian and S. Mehraeen: *Energy* **178** (2019) 33. <https://doi.org/10.1016/j.energy.2019.04.088>
- 4 Y. Liu, H. Khanbareh, M. Halim, A. Feeney, X. Zhang, H. Heidari, and R. Ghannam: *Nano Select* **2** (2021) 1459. <https://doi.org/10.1002/nano.202000242>
- 5 Y. Song, J. Min, Y. Yu, H. Wang, Y. Yang, H. Zhang, and W. Gao: *Sci. Adv.* **6** (2020) eaay9842. <https://www.science.org/doi/full/10.1126/sciadv.aay9842>
- 6 S. Rana, M. Salauddin, M. Sharifuzzaman, S. Lee, Y. Shin, H. Song, S. Jeong, T. Bhatta, K. Shrestha, and J. Park: *Adv. Energy Mater.* **12** (2022) 2202238. <https://doi.org/10.1002/aenm.202202238>
- 7 L. Li, J. Xu, J. Liu, and F. Gao: *Adv. Compos. Hybrid Mater.* **1** (2018) 478. <https://doi.org/10.1007/s42114-018-0046-1>
- 8 H. Katsumura, T. Konishi, H. Okumura, T. Fukui, M. Katsu, T. Terada, T. Umegaki, and I. Kanno: *J. Phys. Conf. Ser.* **1052** (2018) 012060. <https://doi.org/10.1088/1742-6596/1052/1/012060>
- 9 M. Kim, S. Pyo, Y. Oh, Y. Kang, K. Cho, J. Choi, and J. Kim: *Smart Mater. Struct.* **27** (2018) 035001. <https://doi.org/10.1088/1361-665X/aaa722>
- 10 S.-G. Kim, S. Priya, and I. Kanno: *MRS Bull.* **37** (2012) 1039. <https://doi.org/10.1557/mrs.2012.275>
- 11 S. Priya, H.-C. Song, Y. Zhou, R. Varghese, A. Chopra, S.-G. Kim, I. Kanno, L. Wu, D. S. Ha, J. Ryu, and R. G. Polcawich: *Energy Harvesting Syst.* **4** (2017) 3. <https://doi.org/10.1515/ehs-2016-0028>
- 12 R. Harada, N. Iwamoto, S. Kweon, T. Umegaki, and I. Kanno: *Sens. Actuators, A* **322** (2021) 112617. <https://doi.org/10.1016/j.sna.2021.112617>
- 13 C. R. Cho, L. F. Francis, and D. L. Polla: *Mater. Lett.* **38** (1999) 125. [https://doi.org/10.1016/S0167-577X\(98\)00145-1](https://doi.org/10.1016/S0167-577X(98)00145-1)
- 14 Y. Tsujiura, S. Kawabe, F. Kurokawa, H. Hida, and I. Kanno: *Jpn. J. Appl. Phys.* **54** (2015) 10NA04. <https://doi.org/10.7567/JJAP.54.10NA04>